

# Loss of methane and ethene from long-lived gaseous xylum ions (protonated xylene) after “composite” scrambling

Michael Mormann, Dietmar Kuck\*

*Fakultät für Chemie, Universität Bielefeld, Universitätsstraße 25, D-33615 Bielefeld, Germany*

Received 22 January 2002; accepted 18 March 2002

Dedicated to Dr. Yannik Hoppilliard, *une amie*, on the occasion of her 60th birthday.

## Abstract

The unimolecular fragmentation of long-lived gaseous xylum ions,  $\text{CH}_3\text{-C}_6\text{H}_5^+\text{-CH}_3$ , has been studied in detail using  $^{13}\text{C}$ -labeling, in addition to deuterium labeling, in combination with mass-analyzed ion kinetic energy (MIKE) spectrometry. Metastable xylum ions generated from the EI-induced loss of  $\bullet\text{COOR}$  ( $\text{R} = \text{H}, \text{CH}_3$ ) from 1,4-dimethyl-1,4-dihydrobenzoic acid or its methyl ester or by protonation of *para*-xylene under  $\text{Cl}(\text{CH}_4)$  conditions eliminate  $\text{H}_2$ ,  $\text{CH}_4$  and, most remarkably,  $\text{C}_2\text{H}_4$ . The kinetic energy release characteristics of these fragmentation processes are reported.  $^2\text{H}$ -labeling reveals that the loss of methane occurs by protonolytic cleavage of the  $\text{C}^\alpha\text{-C}^{\text{ipso}}$  bonds, excluding intra-complex benzylic hydride abstraction by  $\text{CH}_3^+$  ions.  $^{13}\text{C}$ -labeling confirms the composite scrambling behavior preceding both methane and ethene losses.  $\text{CH}_4$  loss of a major fraction (92%) of xylum ions occurs without C scrambling but with some concomitant hydrogen exchange ( $\text{H}^\alpha/\text{H}^{\text{ring}}$ ) via nonclassical tolylmethonium ions, whereas a minor fraction (8%) undergoes complete C and H scrambling.  $\text{C}_2\text{H}_4$  loss is preceded by different sequences of reversible ring expansion and ring contraction reactions involving methylhydrotropylium ions (protonated methylcycloheptatriene) which, by irreversible ring contraction, eventually form ethylbenzenium ions (protonated ethylbenzene). A major fraction (66–75%) of the ions exhibits “specific” behavior, with the one of the methyl carbons being incorporated specifically into the ethene fragment and the other only after randomization with the carbons of the tolyl unit. A minor fraction (34–25%) of the ions undergoes complete C and H scrambling prior to ethene loss, involving both methyl groups. 1,2- $\text{CH}_3$  shifts are invoked to occur in the xylum and/or dihydrotropylium ions. (Int J Mass Spectrom 219 (2002) 497–514) © 2002 Elsevier Science B.V. All rights reserved.

**Keywords:** Alkylbenzenium ions; Protonated methylbenzenes; Skeletal rearrangements; Scrambling processes; Metastable ions

## 1. Introduction

Protonation of simple, mononuclear aromatic molecules in the gas phase gives rise to arenium ions which are known to be the key intermediates of electrophilic aromatic substitution [1–4]. Benzenium ions, and arenium ions in general, are quite resistant

against skeletal isomerization. The major features of their unimolecular reactivity are the facile and rapid tautomerization by intra-molecular proton shifts [5,6] and the proton-induced fragmentation by heterolytic cleavage of a bond between the ring and a substituent [5,7–9]. The least energy-demanding fragmentation of hetero-functionalized arenium ions  $[\text{ArX} + \text{H}]^+$  is the loss of  $\text{HX}$  ( $\text{X} = \text{F}, \text{Cl}, \text{Br}, \text{I}$ ) [4,10]. Alkylbenzenium ions  $[\text{ArR} + \text{H}]^+$  with  $\text{R} > \text{CH}_3$  generally lose

\* Corresponding author. E-mail: dietmar.kuck@uni-bielefeld.de

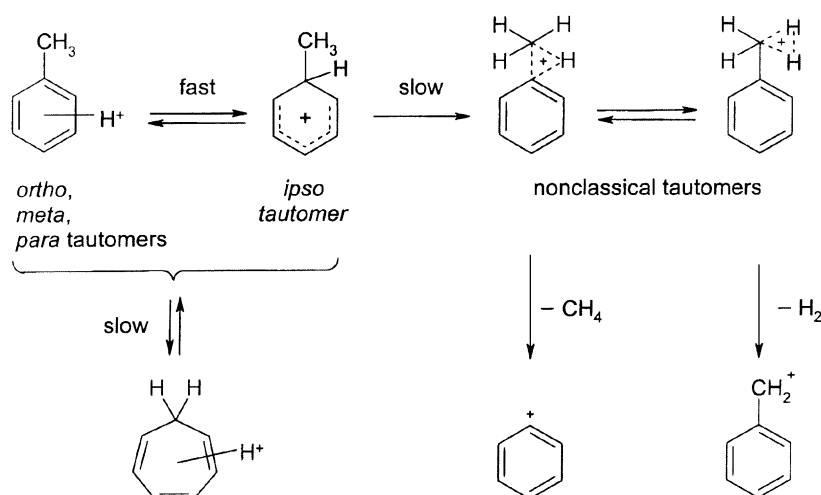
neutral alkenes,  $[R - H]$ , and/or release the corresponding alkyl cations,  $[R]^+$  [4,5a,7–9]. Elimination of the respective alkane,  $[R + H]$ , is observed instead or in competition if an energetically favorable intramolecular hydride abstraction is feasible via the complex  $[ArH R^+]$  [11–13].

Protonated methylbenzenes, such as toluenium and xylenium ions, exhibit a surprisingly complicated fragmentation behavior. Similar to the prototypical benzenium ions, cyclo- $C_6H_7^+$ , they expel a dihydrogen molecule,  $H_2$ , in a highly endothermic reaction [14,15]. However, heterolysis of the  $C^{ipso}-C^\alpha$  bond giving rise to loss of methane was found to compete as another energy-demanding process [15–18]. Deuterium and  $^{13}C$ -labeling revealed that this process is preceded by a set of distinct, deep-seated isomerization processes [15,16], which lead to “composite scrambling” behavior, as discussed recently in a review comprising examples on scrambling processes in gaseous organic ions [6]. In addition, 1,2-methyl shifts have been found to take place in protonated methylbenzenium ions [19,20].

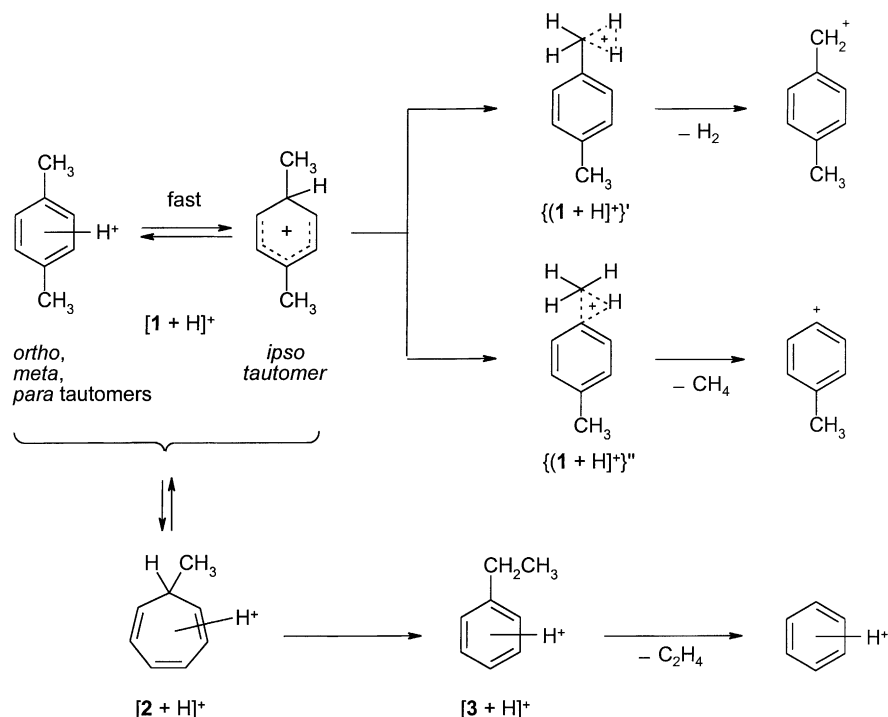
Methane loss from long-lived, metastable toluenium ions comprises a ca. 40% fraction of the ions that undergo reversible ring expansion to dihydrotropylium ions (protonated 1,3,5-cycloheptatriene), leading to randomization of the carbon and hydrogen atoms

prior to formation of phenyl cations and methane (Scheme 1). The remaining 60%-fraction of the metastable ion population undergoes slow and incomplete hydrogen exchange between the methyl and the ring protons ( $H^\alpha/H^{ring}$  scrambling), the latter of which, in turn, are fully equilibrated [6,15]. By contrast to the higher homologues of toluenium ions (*n*-alkylbenzenium ions) mentioned above, protonated xylenes were expected to behave similarly, and a part of the present article reports on a detailed  $^2H$  and  $^{13}C$ -labeling study on the unimolecular elimination of methane from long-lived *para*-xylenium ions,  $[1 + H]^+$  (Scheme 2).

However, there is an additional and unexpected possibility to gain insight into the isomerization of these simple arenium ions. Metastable xylenium ions were found to eliminate ethene, in competition with the losses of  $H_2$  and  $CH_4$  [16]. Whereas the standard  $CI(CH_4)$  mass spectra [17,18] of the xylenes show that this process represents a path of only minute importance for the short-lived  $[1 + H]^+$  ions (Fig. 1a), metastable xylenium ions undergo loss of  $C_2H_4$  to a similar extent (Fig. 1b) as toluenium ions eliminate methane (ca. 11%  $\Sigma$ ). By contrast to methane loss, however, ethene loss indicates directly the occurrence of deep-seated skeletal rearrangement processes in long-lived xylenium ions prior to unimolecular fragmentation (Scheme 2), and another part of this article



Scheme 1. Isomerization and fragmentation of toluenium ions.

Scheme 2. Isomerization and fragmentation of *para*-xylenium ions  $[1 + H]^+$ .

presents a detailed  $^2H$  and  $^{13}C$ -labeling study on the unimolecular elimination of ethene from metastable  $[1 + H]^+$  ions.<sup>1</sup>

## 2. Experimental

### 2.1. Mass spectrometric measurements

The measurements were carried out using double focusing sector-field instruments. The EI/MIKE spectra of ions  $[1a + H]^+$  and  $[1b + H]^+$  generated from the labeled 1,4-dimethyl-1,4-dihydrobenzoic acids (**4a** and **4b**) were performed on a ZAB-2F instrument (Micromass, Manchester, UK) with B/E geometry. Samples were introduced via a septum inlet heated to 170 °C and measured at an accelerating voltage of 8 kV, electron energies of 70 eV, trap current of

100  $\mu A$ , source temperature of 200 °C and nominal ion source pressure of  $1 \times 10^{-7}$  mbar. The CI/MIKE spectra of the  $[M + H]^+$  ions generated from the labeled xylenes **1d–1f** and the  $[M - COOCH_3]^+$  ions generated from methyl 1,4-dimethyl-1,4-dihydrobenzoates (**5c** and **5d**) were measured on an AutoSpec instrument (Fisons, Manchester, UK) with a three-sector EBE geometry. Samples were introduced into the ion source via a heated septum inlet. Methane (Matheson, stated purity > 99.9%) was used as the reactant gas for the CI measurements at a nominal pressure of ca.  $4\text{--}7 \times 10^{-5}$  mbar. The acceleration voltage, electron energy, emission current and source temperature were set to 8 kV, 70 eV, 200  $\mu A$  and  $160 \pm 10$  °C, respectively. The MIKE spectra obtained with the AutoSpec instrument represent the average of at least 200 scans. All relative abundances were calculated from peak areas. The data were corrected for contributions by EI-induced fragmentation of naturally occurring isobaric  $[^{13}C_1]\text{--}M^+$  ions after measurement of the

<sup>1</sup> Similar behavior was found for the adduct ions  $C_8H_{11}^+$  generated by collisional addition of methane to tolyl cations [21].

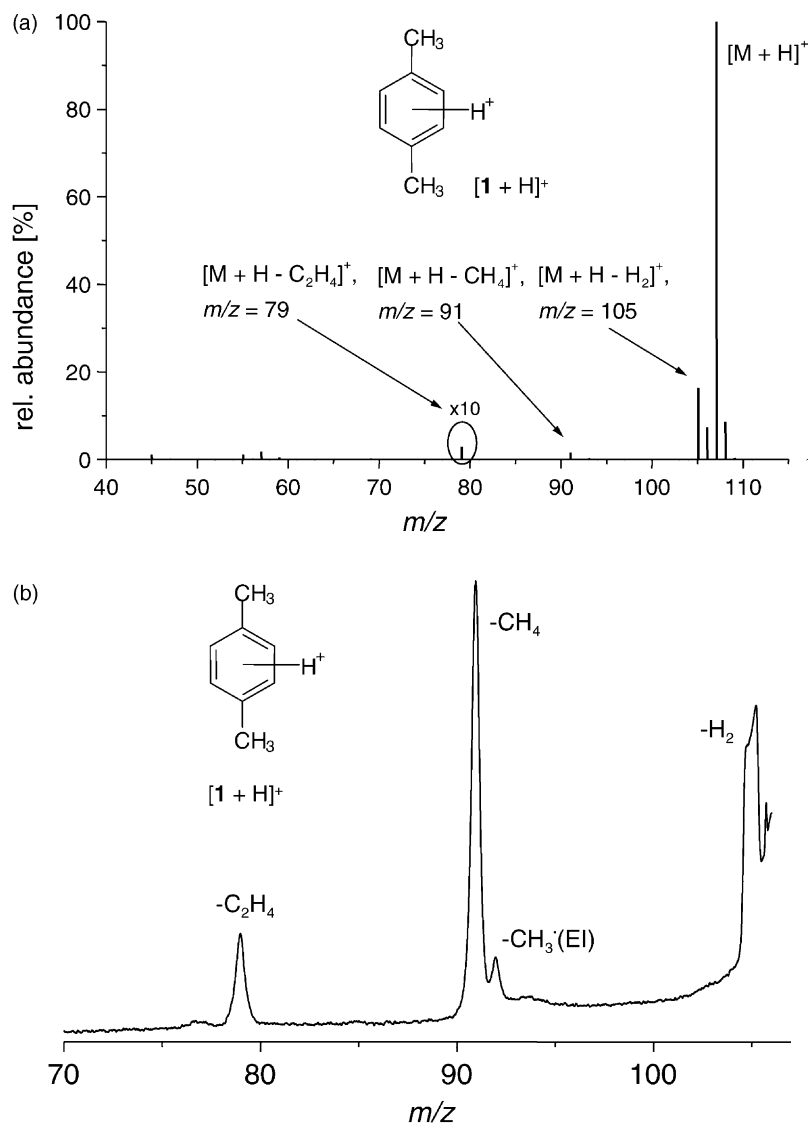


Fig. 1. (a) CI(CH<sub>4</sub>) mass spectrum of *para*-xylene. (b) MIKE spectrum of xylum ions, C<sub>8</sub>H<sub>11</sub><sup>+</sup> ( $m/z$  = 107). The signal at  $m/z$  = 92 in the MIKE spectrum is mainly due to loss of <sup>12</sup>CH<sub>3</sub><sup>•</sup> from isobaric ions [<sup>13</sup>C<sup>12</sup>C<sub>7</sub>H<sub>10</sub>]<sup>•+</sup>.

MIKE spectra of the corresponding [<sup>13</sup>C<sub>0</sub>]-M<sup>•+</sup> ions. The determination of the peak areas was performed by numerical integration. Kinetic energy release (KER) distributions were determined by using the method developed by Szilágyi and Vékey [22]. The KER values given in this paper denote the most probable ( $T^*$ ) and the average ( $\langle T \rangle$ ) values of the kinetic energy released during the respective fragmentation reaction.

## 2.2. Syntheses—general

<sup>1</sup>H NMR spectra were either measured by use of a Bruker DRX 500 (500 MHz) or a Bruker AM 250 (250 MHz) instrument. EI mass spectra were recorded with the VG AutoSpec instrument described above (70 eV). All compounds used were purified by standard procedures, solvents were dried immediately in

most cases. All reactions were carried out under dried argon.

### 2.3. Compounds

#### 2.3.1. [ $\alpha\alpha'$ - $^{13}\text{C}_2$ ]-*para*-Xylene (**1d**)

The synthesis of **1d** was performed by  $\text{Ni}^{\text{II}}$ -catalyzed C–C coupling reaction between [ $^{13}\text{C}$ ]methylmagnesium iodide and 1,4-dichlorobenzene, in analogy to the method described by Tamao et al. [23].

A Grignard solution prepared from [ $^{13}\text{C}$ ]methyl iodide (2.00 g, 13.9 mmol) and magnesium turnings (0.39 g, 16.0 mmol) in 10 mL of diethyl ether was added dropwise to a stirred solution of 1,4-dichlorobenzene (0.80 g, 5.4 mmol) and [1,2-bis(diphenylphosphine)ethane]nickel(II) chloride (30.9 mg, 0.058 mmol) in 10 mL of diethyl ether at 0 °C. The reaction mixture was stirred for additional 10 min at 0 °C and then heated under reflux for 24 h. After hydrolysis with diluted aqueous hydrochloric acid (2 N) the organic layer was separated and the aqueous layer was extracted five times with *n*-pentane. The combined organic layers were dried over sodium sulfate and the solvents were removed by careful distillation using a 30 cm Vigreux column. Fractionated distillation of the residue afforded **1d** (408 mg, 70%) as a colorless liquid; bp: 136 °C;  $^1\text{H}$  NMR (500 MHz,  $\text{CDCl}_3$ ):  $\delta$  = 7.06 (br, s, 4H), 2.31 (d,  $J(^1\text{H}, ^{13}\text{C})$  = 125.8 Hz, 6H); MS (EI, 70 eV):  $m/z$  = 108 (62,  $\text{M}^{\bullet+}$ ), 107 (33), 93 (24), 92 (100), 79 (9), 78 (7), 52 (9), 51 (6).

#### 2.3.2. [ $1\text{-}^{13}\text{C}$ ]-*para*-Xylene (**1e**)

This [*ipso*- $^{13}\text{C}$ ]-labeled *p*-xylene was prepared in a multistep synthesis via [ $1\text{-}^{13}\text{C}$ ]-1,4-dimethylcyclohexanol as an intermediate product, in analogy to the synthesis of [ $1\text{-}^{13}\text{C}$ ]toluene described by Fields et al. [24] and modified by Robertson and Djerassi [25]. The details of the synthesis have been published elsewhere [26]. The final product was contaminated by the corresponding dimethylcyclohexanes (ca. 6%).  $^1\text{H}$  NMR of **1e** (500 MHz,  $\text{CDCl}_3$ ):  $\delta$  = 7.06 (br, s, 4H), 2.31 (d,  $J(^1\text{H}, ^{13}\text{C})$  = 5.5 Hz, 3H), 2.31 (s, 3H); MS (EI, 70 eV):  $m/z$  = 107 (59,  $\text{M}^{\bullet+}$ ), 106 (36), 92 (100), 91

(16), 79 (7), 78 (12), 77 (5), 66 (5), 65 (4), 52 (7), 51 (9).

#### 2.3.3. [ $2\text{-}^{13}\text{C}$ ]-*para*-Xylene (**1f**)

This [*ortho*- $^{13}\text{C}$ ]-labeled *p*-xylene was prepared by a similar synthesis sequence as described for **1e** using ethyl [ $^{13}\text{C}$ ]formate as the  $^{13}\text{C}$ -containing building block and 1,5-dibromo-2-methylhexane as starting material for the six-membered cyclization and via [ $1\text{-}^{13}\text{C}$ ]-2,5-dimethylcyclohexanol as an intermediate product. The details of the synthesis have also been published elsewhere [26]. The final product was again contaminated by the related dimethylcyclohexanes (ca. 6%).  $^1\text{H}$  NMR of **1f** (500 MHz,  $\text{CDCl}_3$ ):  $\delta$  = 7.06 (s, 3H, H), 7.04 (dd,  $J(^1\text{H}, ^{13}\text{C})$  = 155.8 Hz,  $J(^1\text{H}, ^1\text{H})$  = 8.2 Hz, 1H), 2.29 (s, 6H); MS (EI, 70 eV):  $m/z$  = 107 (56,  $\text{M}^{\bullet+}$ ), 106 (33), 92 (100), 91 (14), 80 (6), 79 (7), 78 (11), 77 (5), 66 (5), 65 (3), 52 (6), 51 (6), 40 (8) 39 (10).

#### 2.3.4. [ $\text{D}_3$ ]-labeled 1,4-dimethyl-1,4-dihydrobenzoic acids (**4a** and **4b**)

4-Methyl-1-trideuteromethyl-1,4-dihydrobenzoic acid (**4a**) and 1-methyl-4-trideuteromethyl-1,4-dihydrobenzoic acid (**4b**) were synthesized by Birch reduction of *para*-toluic acid and *para*-[methyl- $\text{D}_3$ ]toluic acid and subsequent quenching with [ $\text{D}_3$ ]methyl iodide and methyl iodide, respectively. The isotopic purity of **4a** was >99%  $\text{d}_3$  and the label was located specifically in the 1-methyl group. The [ $\text{D}_3$ ]-labeled *para*-toluic acid used for the synthesis of **4b** was prepared by repeated H/D exchange of *para*-toluic acid with KOD/ $\text{D}_2\text{O}$  and was found (by mass spectrometry) to consist of a mixture of isotopomers ( $\text{d}_2$  6%,  $\text{d}_3$  81%,  $\text{d}_4$  10%,  $\text{d}_5$  3%).  $^1\text{H}$  NMR spectrometry revealed that the label was incorporated partially into the positions 3 and 5 of the ring and in part at the expense of the methyl labeling. Subsequent Birch reduction furnished acid **4b** with a similar distribution of isotopomers.

#### 2.3.5. $^{13}\text{C}$ -Labeled methyl 1,4-dimethyl-1,4-dihydrobenzoates (**5c** and **5d**)

In analogy to the synthesis of 1-([ $^{13}\text{C}$ ]methyl)-1,4-dihydrobenzoic acid described previously [15,27],

these compounds were obtained by Birch reduction of the *para*-toluic acid and [ $^{13}\text{C}$ -methyl]toluic acid, respectively, using lithium in liquid ammonia, and subsequent quenching with [ $^{13}\text{C}$ ]methyl iodide or unlabeled methyl iodide, respectively. The 1,4-dimethyl-1,4-dihydrobenzoic acids (**4c** and **4d**), thus obtained were converted into the corresponding methyl esters **5c** and **5d** by reaction with diazomethane in diethyl ether.

**2.3.5.1. 1-[ $^{13}\text{C}$ ]Methyl-4-methyl-1,4-dihydrobenzoate (4c).** 1-[ $^{13}\text{C}$ ]Methyl-4-methyl-1,4-dihydrobenzoic acid was prepared from *para*-toluic acid (0.40 g, 3.0 mmol) and lithium metal (0.10 g, 10 mmol) in liquid ammonia and subsequent quenching with [ $^{13}\text{C}$ ]methyl iodide (0.65 g, 4.5 mmol) as a colorless oil (yield 35%), bp 140 °C/0.1 mbar.  $^1\text{H}$  NMR (250 MHz,  $\text{CDCl}_3$ ):  $\delta$  = 10.32 (br, s, 1H), 5.75–5.82 (m, 4H), 2.70–2.81 (m, 1H), 1.38 (d,  $J(^1\text{H}, ^{13}\text{C})$  = 130.0 Hz, 2H), 1.36 (d,  $J(^1\text{H}, ^{13}\text{C})$  = 123.6 Hz, 1H), 1.09 (d,  $J$  = 7.3 Hz, 3H); MS (EI, 70 eV):  $m/z$  = 153 (8,  $\text{M}^+$ ), 108 (100), 107 (12), 106 (17), 92 (56), 91 (61).

**2.3.5.2. Methyl 1-[ $^{13}\text{C}$ ]methyl-4-methyl-1,4-dihydrobenzoate (5c).** Treatment of acid **4c** (0.10 g, 0.65 mmol) with diazomethane in diethyl ether gave **5c** as a colorless oil (yield 83%); bp 105 °C/40 mbar.  $^1\text{H}$  NMR (250 MHz,  $\text{CDCl}_3$ ):  $\delta$  = 5.68–5.76 (m, 4H), 3.68 (s, 3H), 2.63–2.73 (m, 1H), 1.34 (d,  $J(^1\text{H}, ^{13}\text{C})$  = 129.8 Hz, 2H), 1.33 (d,  $J(^1\text{H}, ^{13}\text{C})$  = 125.6 Hz, 1H), 1.08 (d,  $J$  = 7.3 Hz, 3H); MS (EI, 70 eV):  $m/z$  = 167 (5,  $\text{M}^+$ ), 150 (14), 119 (37), 108 (100), 107 (33), 106 (25), 92 (64), 91 (76), 80 (11), 79 (12), 78 (12), 77 (14), 66 (11), 65 (29), 59 (14), 51 (14), 41 (10), 39 (22).

**2.3.5.3. 1,4-(Di[ $^{13}\text{C}$ ]methyl)-1,4-dihydrobenzoate (4d).** Benzene[ $^{13}\text{C}$ ]carboxylic acid was prepared by carboxylation of phenylmagnesium bromide with [ $^{13}\text{C}$ ]carbon dioxide and reduced stepwise with lithium aluminum hydride to [ $\alpha$ - $^{13}\text{C}$ ]benzyl alcohol followed by chloralane reduction to [ $\alpha$ - $^{13}\text{C}$ ]toluene according to the method described by Brewster et al.

[28]. [ $\alpha$ - $^{13}\text{C}$ ]Toluene was converted into a mixture of *ortho*- and *para*-bromo-[ $\alpha$ - $^{13}\text{C}$ ]toluenes using dioxane dibromide [29]. Metallation of the mixture with *n*-butyllithium followed by reaction with carbon dioxide using the procedure by Gilman et al. [30] furnished pure 4-[ $^{13}\text{C}$ ]methylbenzoic acid after crystallization from water. 1,4-(Di[ $^{13}\text{C}$ ]methyl)-1,4-dihydrobenzoic acid (**4d**) was prepared as described above for **4c** by Birch reduction and quenching with [ $^{13}\text{C}$ ]methyl iodide, yield 45%, bp 150 °C/0.08 mbar.  $^1\text{H}$  NMR (250 MHz,  $\text{CDCl}_3$ ):  $\delta$  = 10.34 (br, s, 1H), 5.75–5.82 (m, 4H), 2.72–2.79 (m, 1H), 1.37 (d,  $J(^1\text{H}, ^{13}\text{C})$  = 129.9 Hz, 2H), 1.36 (d,  $J(^1\text{H}, ^{13}\text{C})$  = 130.0 Hz, 1H), 1.10 (dd,  $J(^1\text{H}, ^{13}\text{C})$  = 127.5 Hz,  $J(^1\text{H}, ^1\text{H})$  = 7.3 Hz, 3H); MS (EI, 70 eV):  $m/z$  = 154 (6,  $\text{M}^+$ ), 109 (100), 108 (10), 107 (18), 93 (53), 92 (65).

**2.3.5.4. Methyl 1,4-(di[ $^{13}\text{C}$ ]methyl)-1,4-dihydrobenzoate (5d).** This compound was obtained by reaction of **4d** with diazomethane in diethyl ether, as outlined above, as a colorless oil, yield 90%, bp 115 °C/50 mbar;  $\delta$  = 5.72 (br, s, 4H), 3.68 (s, 3H), 2.65–2.73 (m, 1H), 1.33 (d,  $J(^1\text{H}, ^{13}\text{C})$  = 129.7 Hz, 2H), 1.32 (d,  $J(^1\text{H}, ^{13}\text{C})$  = 129.6 Hz, 1H), 1.09 (dd,  $J(^1\text{H}, ^{13}\text{C})$  = 127.3 Hz,  $J(^1\text{H}, ^1\text{H})$  = 7.3 Hz, 3H); MS (EI, 70 eV):  $m/z$  = 168 (4,  $\text{M}^+$ ), 151 (15), 120 (37), 109 (100), 108 (30), 107 (25), 93 (26), 92 (76), 81 (6), 80 (13), 79 (10), 78 (9), 66 (17), 65 (10), 59 (11), 51 (8), 40 (12), 39 (10).

### 3. Results and discussion

#### 3.1. Fragmentation of xylum ions

The  $\text{CI}(\text{CH}_4)$  mass spectrum of *para*-xylene (**1**) reflects the stability of gaseous xylum ions (Fig. 1a). In agreement with previous results [17,18], the major fragmentation is loss of  $\text{H}_2$  ( $m/z$  = 105), occurring to ca. 15% B only, and loss of  $\text{CH}_4$  ( $m/z$  = 91), amounting to ca. 3% B. Under the conditions used in the present study, loss of  $\text{C}_2\text{H}_4$  ( $m/z$  = 79) takes place with relative abundances of 0.5–1% B

only. In one of the previous reports,  $\text{Cl}(\text{H}_2)$  was required to induce a notable peak at  $m/z = 79$  [17].

The MIKE spectrum of  $\text{C}_8\text{H}_{11}^+$  ions, generated by either protonation of *para*-xylene or by EI-induced fragmentation of 1,4-dimethyl-1,4-dihydrobenzoic acid (**4**) or its methyl ester [16,31,32],<sup>2</sup> exhibits signals for the losses of  $\text{H}_2$  and  $\text{CH}_4$  in similar extents (ca. 45%  $\Sigma$  each) (Fig. 1b). The loss of  $\text{C}_2\text{H}_4$  contributes considerably more (9–11%  $\Sigma$ ) as compared to the standard  $\text{Cl}(\text{CH}_4)$  mass spectrum. As known from many other dihydrogen losses including that from protonated toluene, the elimination of  $\text{H}_2$  is accompanied by the release of large amounts of kinetic energy ( $T^* = 1.178 \text{ eV}$ ,  $\langle T \rangle = 1.238 \text{ eV}$ , see Section 2 [22]).<sup>3</sup> It has been proposed [15] that, in contrast to previous suggestions [14], the loss of  $\text{H}_2$  from toluenium ions may occur via the nonclassical phenylmethonium ion, generating  $\text{C}_7\text{H}_7^+$  ions as benzyl cations (cf. Scheme 1). Correspondingly, xylenium ions may lose  $\text{H}_2$  via tolylmethonium intermediates  $\{[\mathbf{1} + \text{H}]^+\}'$  (Scheme 2). In both cases, a relatively high activation barrier has to be surmounted before releasing the neutral fragment along a highly exothermic reaction path. The mechanism and dynamics of this kind of concerted bond reorganization prior to  $\text{H}_2$  expulsion from small protonated organic molecules have been treated in detail recently [33–36]. In view of the minor overall importance of skeletal rearrangements of the xylenium ions prior to the mechanistically related methane loss, dihydrogen loss via ring-expanded methyl-dihydro-tropylium ions  $[\mathbf{2} + \text{H}]^+$  appears unlikely. This is in agreement with the experimental finding that protonated methylcycloheptatriene  $[\mathbf{2} + \text{H}]^+$  loses  $\text{H}_2$  subsequent to ring contraction to xylenium ions [37].

<sup>2</sup> The MIKE spectra of ions  $[\mathbf{1} + \text{H}]^+$  generated by either method were found to be virtually identical, e.g.,  $[\text{H}_2]:[\text{CH}_4]:[\text{C}_2\text{H}_4] = 47:41:12$  by CI of **1** and  $[\text{H}_2]:[\text{CH}_4]:[\text{C}_2\text{H}_4] = 44:45:11$  by EI of **4**. As a notable advantage, use of the methyl ester **5** of acid **4** allows one to perform the measurements at lower temperatures.

<sup>3</sup> It is noted that the  $T^*$  and  $\langle T \rangle$  values for  $\text{H}_2$  loss from ions  $[\mathbf{1} + \text{H}]^+$  and for  $\text{C}_2\text{H}_4$  loss from ions  $[\mathbf{2} + \text{H}]^+$  published by us in [37] are incorrect.

The loss of  $\text{CH}_4$  from xylenium ions gives rise to signals with Gaussian peak shapes. The kinetic energy release associated with this process is relatively small ( $T^* = 32.6 \text{ meV}$ ,  $\langle T \rangle = 92.4 \text{ meV}$ ) and similar to that of the methane loss from toluenium ions [15], but still higher than that associated with the C–C bond cleavages of protonated higher alkylbenzenes [8]. Similar to the  $\text{CH}_4$  loss, elimination of  $\text{C}_2\text{H}_4$  from xylenium ions is accompanied by small amounts of kinetic energy ( $T^* = 12.3 \text{ meV}$ ,  $\langle T \rangle = 49.9 \text{ meV}$ ) and in line with the characteristics found for the isomeric ethylbenzenium ions ( $T^* = 13.9 \text{ meV}$ ,  $\langle T \rangle = 35.2 \text{ meV}$  [38],  $T_{0.5} = 28 \text{ meV}$  [39]) and protonated methylcycloheptatriene ( $T^* = 16.5 \text{ meV}$ ,  $\langle T \rangle = 51.4 \text{ meV}$ ) [38].

### 3.2. Methane loss from labeled xylenium ions

When 1- $[\text{D}_3]$ methyl-4-methyl-1,4-dihydrobenzoic acid (**4a**) is ionized under EI conditions, the losses of the  $\bullet\text{CO}_2\text{H}$  radical generates  $[\alpha,\alpha,\alpha\text{-D}_3]$ -labeled *para*-xylenium ions  $[\mathbf{1a} + \text{H}]^+$ . The same ions are formed from 4- $[\text{D}_3]$ methyl-1-methyl-1,4-dihydrobenzoic acid (**4b**), which is evident from its nearly identical fragmentation behavior (Fig. 2).<sup>4</sup> Loss of  $\bullet\text{CO}_2\text{CH}_3$  from the corresponding methyl esters yield exactly the same results [16]. The MIKE spectra of ions  $[\mathbf{1a} + \text{H}]^+$  exhibit predominant loss of  $\text{CH}_4$  and  $\text{CHD}_3$  in a ratio of 10:7 and only minor contributions of  $\text{CH}_3\text{D}$  and  $\text{CH}_2\text{D}_2$ . At first glance, the abundance pattern of the methane isotopomers suggests a composite scrambling behavior, that is, the competition of some specific fragmentation and some non-specific fragmentation after extended H/D exchange [6]. The fact that the elimination is independent of the regiospecific labeling of the neutral precursor reflects the symmetrization of the xylenium ions  $[\mathbf{1a} + \text{H}]^+$  by the well-known fast proton ring walk in protonated arenes [5a,6].

<sup>4</sup> The slightly higher relative intensities at the higher masses within the peak groups for  $\text{C}(\text{H},\text{D})_4$  and  $\text{C}_2(\text{H},\text{D})_4$  loss in the MIKE spectrum of ions  $[\mathbf{4b} - \text{CO}_2\text{H}]^+$  (Fig. 2b), as compared to the spectrum of ions  $[\mathbf{4a} - \text{CO}_2\text{H}]^+$  (Fig. 1a) is due to the partial incorporation of the label into the ring instead of the 4-methyl group.



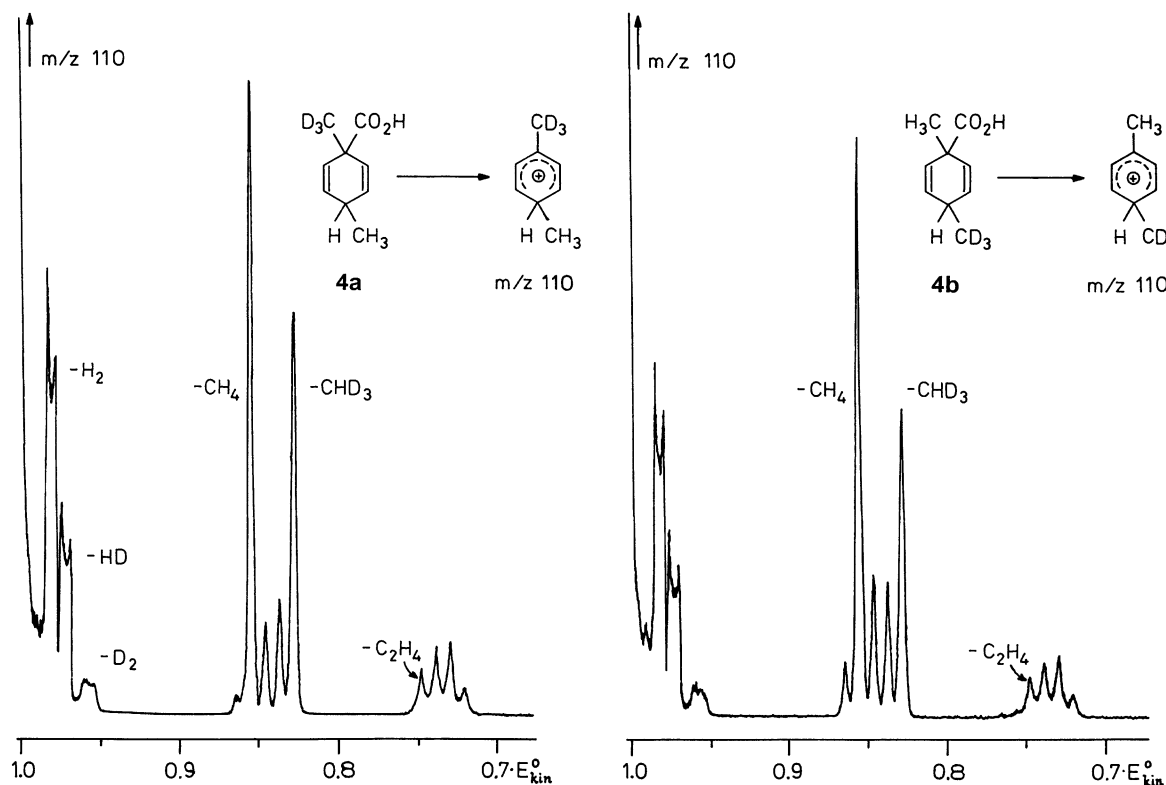


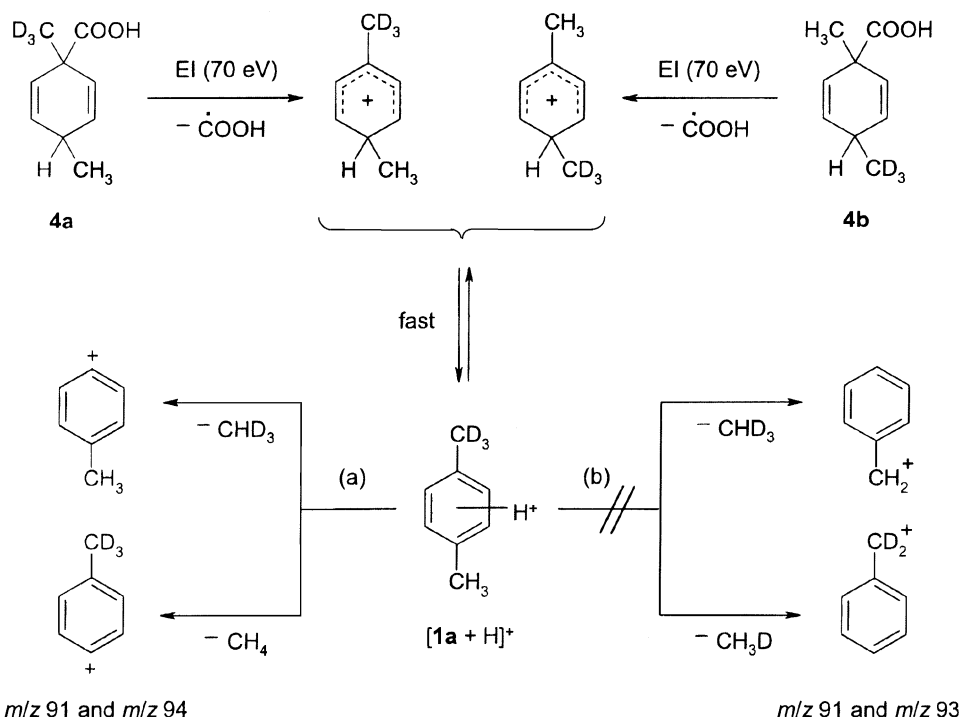
Fig. 2. MIKE spectra of  $[\alpha, \alpha, \alpha\text{-D}_3]\text{-xylenium ions}$ ,  $\text{C}_8\text{H}_8\text{D}_3^+$  ( $m/z = 110$ ) generated by EI-induced loss of  $\bullet\text{COOH}$  from the labeled 1,4-dimethyl-1,4-dihydrobenzoic acids (**4a** and **4b**). Note that the energy (and mass) scale runs from the left to the right here (cf. Section 2) (footnote 4).

The results of the deuterium labeling experiments allow us to distinguish between several cases for the fragmentation of ions  $[\mathbf{1} + \text{H}]^+$ : (i) Specific loss of the elements of the methyl groups together with one of the five equilibrating ring hydrogens (Scheme 3, path a). This process appears to be dominant but not the only one. (ii) Complete skeletal scrambling of the  $\text{C}_8\text{H}_{11}^+$  ions, rendering all of the 11 hydrogen atoms equivalent. This situation can be excluded because the experimental data are far different from the “statistical” pattern (Table 1). (iii) Specific loss of the elements of one methyl group together with a hydrogen atom from the other one (Scheme 3, path b). In that case, a methyl cation would be released into an ion/neutral complex  $[\text{CH}_3\text{C}_6\text{H}_5 \text{ CH}_3^+]$ , which would collapse by exothermic transfer of the hydride from the remaining methyl group to the methyl cation.

This alkane loss channel, which is known to occur with (*tert*-butyl)-substituted alkylbenzenium ions [11–13] and protonated ethers [40,41], does not occur at significant relative rates because loss of  $\text{CH}_3\text{D}$  leading to ions  $m/z = 92$  represents a minor contribution only. Obviously, formation of the complex  $[\text{CH}_3\text{C}_6\text{H}_5 \text{ CH}_3^+]$  is not viable for energetic reasons [11c]. It will be shown below that the methane loss from ions  $[\mathbf{1a} + \text{H}]^+$  can be explained by a combination of the specific process (i) and the random one (ii).

Three  $^{13}\text{C}$ -labeled xylenes (**1d–1f**) and two  $^{13}\text{C}$ -labeled methyl 1,4-dimethyl-1,4-dihydrobenzoates (**5c** and **5d**) were synthesized and the MIKE spectra of the corresponding xylenium ions measured to elucidate the mechanism of the methane and ethene elimination. The partial MIKE spectra reflecting the methane





Scheme 3. Generation of  $[\alpha,\alpha,\alpha\text{-D}_3]$ -labeled xylenium ions  $[\mathbf{1a} + \text{H}]^+$  by EI-induced dissociation of 1,4-dimethyl-1,4-dihydrobenzoic acids (**4a** and **4b**) and two a priori possibilities for the mechanism of methane loss (see text).

loss are reproduced in Fig. 3 and the data collected in Table 2.

In all cases studied, the methane lost is almost completely carbon-specific: it contains almost exclusively the carbon atoms of the original methyl

Table 1  
Loss of methane from metastable xylenium ions  $\text{CD}_3\text{-C}_6\text{H}_5\text{-CH}_3$  ( $[\mathbf{1a} + \text{H}]^+$ )<sup>a</sup>

Entry/loss of	$\text{CHD}_3$	$\text{CH}_2\text{D}_2$	$\text{CH}_3\text{D}$	$\text{CH}_4$
Experimental <sup>b</sup>	<b>34.8</b>	<b>9.0</b>	<b>6.8</b>	<b>49.4</b>
Statistical ( $\text{H}_8/\text{D}_3$ )	2.4	25.5	50.9	21.2
Composite model <sup>c</sup>	46.2	2.0	4.1	47.7
"Specific" fraction (92%) <sup>d</sup>	46.0	0	0	46.0
"Statistical" fraction (8%)	0.2	2.0	4.1	1.7
Deviation (due to $\text{H}^\alpha/\text{H}^{\text{ring}}$ exchange) <sup>e</sup>	-11.4	+7.0	+2.7	+1.7

<sup>a</sup> Data given in %  $\Sigma$ .

<sup>b</sup> Precursor ion:  $\mathbf{4a}^{+\bullet}$ .

<sup>c</sup> See text.

<sup>d</sup> Neglecting isotope effects.

<sup>e</sup> Difference between experimental and model data.

groups. However, there is a significant predominance (54:46) for the loss of  $\text{CH}_4$  over that of  $^{13}\text{CH}_4$  from the singly  $[\alpha\text{-}^{13}\text{C}]$ -labeled ions  $[\mathbf{1c} + \text{H}]^+$ , indicating some contribution from the ring. The doubly labeled  $[\alpha\text{-}^{13}\text{C}]$ -isotopomer  $[\mathbf{1d} + \text{H}]^+$  expels only 5% of the total methane as  $^{12}\text{CH}_4$ . Complementarily, the two  $[\text{ring-}^{13}\text{C}]$ -labeled isotopomers  $[\mathbf{1e} + \text{H}]^+$  and  $[\mathbf{1f} + \text{H}]^+$  both eliminate only ca. 1% of  $^{13}\text{CH}_4$ .

Careful analysis of the  $^{13}\text{C}$ -labeling data confirms that a major fraction of the xylenium ions expels methane without skeletal rearrangement but that a minor fraction undergoes ring expansion, in analogy to toluenium ions. The ratio  $[\text{CH}_4]:[^{13}\text{CH}_4] = 1.29$  observed for ions  $[\mathbf{1c} + \text{H}]^+$  exceeds by far any conceivable kinetic isotope effect [42] and, in fact, the minor but significant loss of  $\text{CH}_4$  from ions  $[\mathbf{1d} + \text{H}]^+$  leaves only partial scrambling as the origin for the behavior of ions  $[\mathbf{1c} + \text{H}]^+$ .

Several models involving composite scrambling behavior have been considered [38b]. In the best-fitting

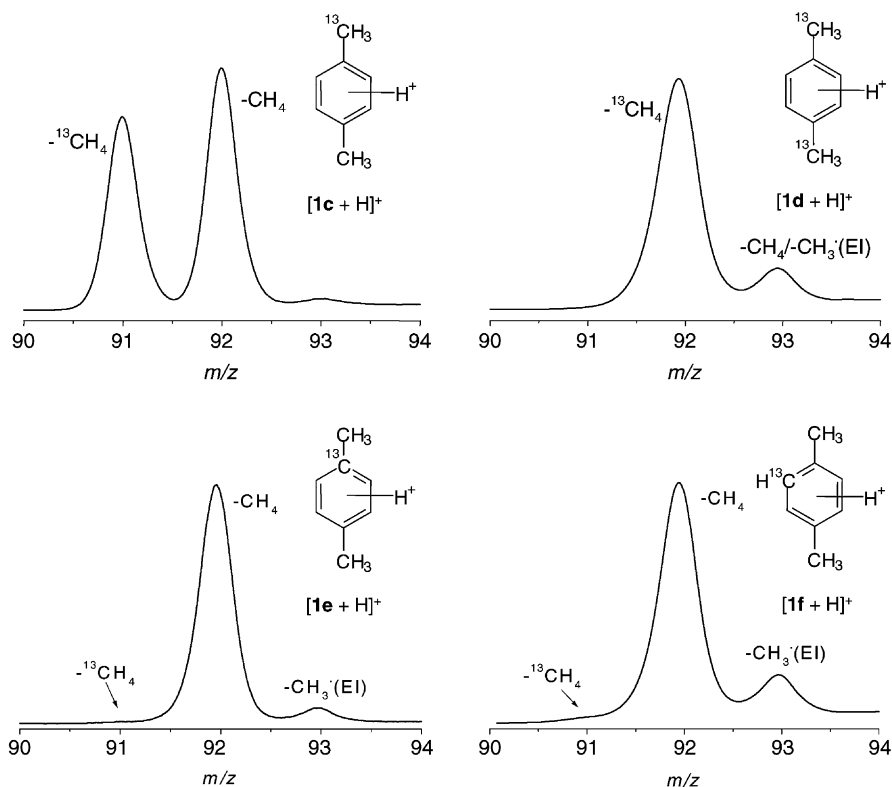


Fig. 3. Partial MIKE spectra of the  $^{13}\text{C}$ -labeled xylenium ions  $[\mathbf{1c} + \text{H}]^+ - [\mathbf{1f} + \text{H}]^+$  showing the loss of methane. Ions  $[\mathbf{1c} + \text{H}]^+$  were generated by EI of methyl 1- $^{13}\text{C}$  methyl-4-methyl-1,4-dihydrobenzoate (**5c**), whereas ions  $[\mathbf{1d} + \text{H}]^+ - [\mathbf{1f} + \text{H}]^+$  were generated by CI( $\text{CH}_4$ ) from the corresponding  $^{13}\text{C}$ -labeled xylenes. The major parts of the signals at  $m/z = 93$  are due to EI-induced fragmentation (cf.  $m/z = 92$ , Fig. 1b).

Table 2

Loss of methane from metastable  $^{13}\text{C}$ -labeled xylenium ions  $[\mathbf{1c} + \text{H}]^+ - [\mathbf{1f} + \text{H}]^+{}^a$

Ion		Neutral precursor	Loss of $^{13}\text{CH}_4$	Loss of $^{12}\text{CH}_4$
$^{13}\text{CH}_3\text{-C}_6\text{H}_5^+ - \text{CH}_3$ $[\mathbf{1c} + \text{H}]^+$	Exp'1	<b>5c</b> (EI)	<b>45.6</b>	<b>54.4</b>
Specific loss ( $\alpha$ - and $\alpha'$ -C)			50.0	50.0
Statistical loss ( $^{13}\text{C}_1/^{12}\text{C}_7$ )			12.5	87.5
Composite model <sup>b</sup>			47.0	53.0
$^{13}\text{CH}_3\text{-C}_6\text{H}_5^+ - ^{13}\text{CH}_3$ $[\mathbf{1d} + \text{H}]^+$	Exp'1	<b>5d</b> (EI) <b>1d</b> (CI)	<b>95.5</b> <b>95.5</b>	<b>4.5</b> <b>4.5</b>
Specific loss ( $\alpha$ - and $\alpha'$ -C)			100.0	0
Statistical loss ( $^{13}\text{C}_2/^{12}\text{C}_6$ )			25.0	75.0
Composite model <sup>b</sup>			94.0	6.0
$[1\text{-}^{13}\text{C}]\text{-}\{\text{CH}_3\text{-C}_6\text{H}_5^+ - \text{CH}_3\}$ $[\mathbf{1e} + \text{H}]^+$	Exp'1	<b>1e</b> (CI)	<b>0.9</b>	<b>99.1</b>
$[2\text{-}^{13}\text{C}]\text{-}\{\text{CH}_3\text{-C}_6\text{H}_5^+ - \text{CH}_3\}$ $[\mathbf{1f} + \text{H}]^+$	Exp'1	<b>1f</b> (CI)	<b>1.5</b>	<b>98.5</b>
Specific loss ( $\alpha$ - and $\alpha'$ -C)			0	100.0
Statistical loss ( $^{13}\text{C}_1/^{12}\text{C}_7$ )			12.5	87.5
Composite model <sup>b</sup>			1.0	99.0

<sup>a</sup> Data given in %  $\Sigma$ .

<sup>b</sup> Calculated for composite scrambling (92% specific, 8% statistical), see text.

one, a 92%-fraction of the metastable xylenium ions is assumed to undergo specific loss of a methyl group by protonolysis without any preceding ring expansion/contraction. Although not relevant for the methane loss within this model, it is reasonable to assume skeletal isomerization by 1,2-shifts of the methyl groups (methyl ring walk), generating a mixture of isomeric xylenium ions and rendering all ring carbon atoms equivalent. Methyl shifts in ions  $[1 + H]^+$  have been shown to occur under radiolysis [19] and  $Cl(CH_4)$  conditions [20]. In solution, they require similar or only gradually higher activation energies than comparable 1,2-H shifts.<sup>5</sup> Thus, the critical energies of 1,2-CH<sub>3</sub> shifts in ions  $[1 + H]^+$  are certainly much lower than the thermochemical threshold of methane loss ( $<70 \text{ kJ mol}^{-1}$  vs. ca.  $235 \text{ kJ mol}^{-1}$ ) [5b,45].<sup>6</sup> A minor fraction of 8% of the xylenium ions is assumed to undergo reversible ring expansion to methyldihydrotropylium ions  $[2 + H]^+$ , producing a mixture of isomeric xylenium ions with all carbons being randomized. As shown in Table 2, this model matches the experimental data of all of the four isotopomeric xylenium ions  $[1c + H]^+ - [1f + H]^+$  satisfactorily and certainly within the limits of experimental error ( $\pm 2\%$ ).

When the 92:8 ratio is used as a basis to simulate the elimination of  $C(H,D)_4$  from the  $[\alpha,\alpha,\alpha-D_3]$ -labeled xylenium ions  $[1a + H]^+$ , the abundance distribution is only in qualitative agreement with the pattern obtained experimentally (Table 1). Whereas the relative amount of  $CH_4$  lost (47.7%) is close to the experimental value, the amount of  $CHD_3$  expected by the model exceeds the observed contribution by ca. 11%. In turn, the observed losses of  $CH_2D_2$  and  $CH_3D$  are considerably higher than those expected from the model. Therefore, a slow and incomplete H/D exchange between the  $[D_3]$ -methyl group and the ring hydrogen atoms has to be assumed, generating ca. 7% of  $CH_2D_2$  and ca. 3% of  $CH_3D$  in excess of the same methane isotopomers which are released from

the 8%-fraction of ions which undergo complete C and H scrambling by the reversible skeletal rearrangement. Thus, of the 92%-fraction reacting by carbon-specific methane loss, a sub-fraction of ca. 10% (per methyl group) undergoes the slow  $H^\alpha/H^{\text{ring}}$  exchange.

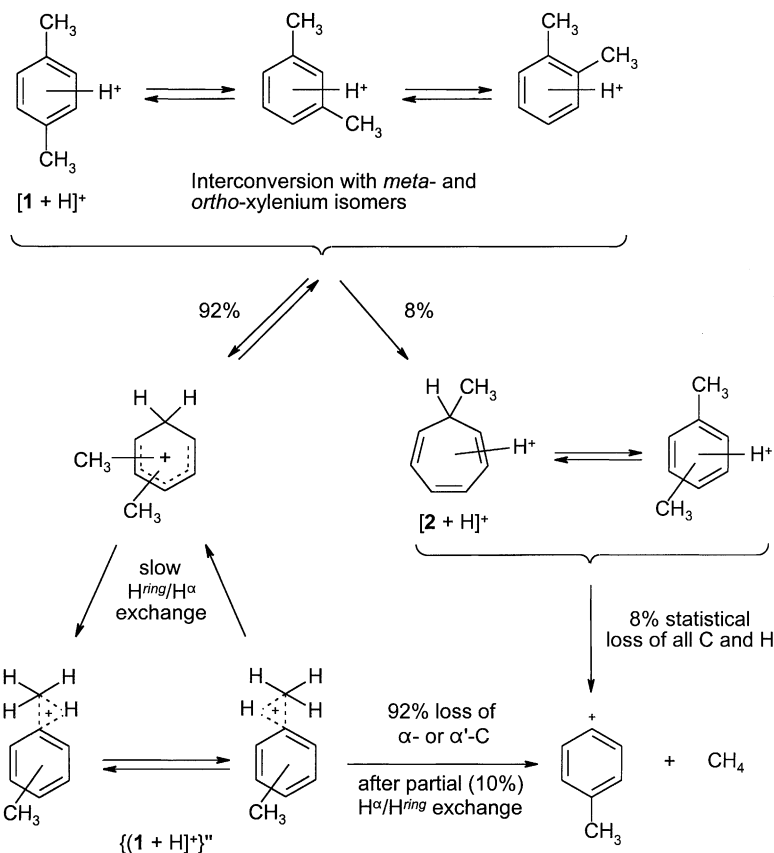
This composite mechanistic picture is in analogy to the reactivity of the metastable toluenium ions [15]. Similar to those, the major fraction of metastable ions expels methane in a carbon-specific manner but with significantly reduced hydrogen retention. A minor fraction of the ions suffer complete carbon and hydrogen scrambling prior to methane loss. In the case of metastable toluenium ions, a 60%-fraction was found to react by C-specific methane loss, including one-third of these ions (20%) which undergo slow  $H^\alpha/H^{\text{ring}}$  exchange, and the remaining 40%-fraction was found to undergo complete C and H scrambling. For xylenium ions  $[1 + H]^+$ , the overall specificity is higher: a 92%-fraction reacts by C-specific methane loss including, in total, a 20%-fraction of ions undergoing the slow  $H^\alpha/H^{\text{ring}}$  exchange, and only an 8%-fraction of the ions suffer complete C and H scrambling (Scheme 4).

### 3.3. Ethene loss from labeled xylenium ions

The elimination of ethene from metastable xylenium ions occurs after profound hydrogen scrambling. This is evident from Fig. 2, which shows a convex pattern for the loss of ethene isotopomers in contrast to the concave pattern for the partially specific loss of methane isotopomers. The observation that H/D exchange in ions  $[1a + H]^+$  is more progressed prior to  $C_2(H,D)_4$  loss than prior to  $C(H,D)_4$  loss agrees with expectation since the former process necessarily requires deep-seated skeletal rearrangement whereas the latter does not. However, the abundance distribution of  $C_2(H,D)_4$  isotopomers expelled from ions  $[1a + H]^+$  clearly does not reach the pattern calculated for complete randomization (Table 3). Again, a thorough inspection of the results of  $^{13}C$ -labeling was necessary to trace the observed hydrogen exchange to a reasonable but rather complex mechanistic picture. The partial spectra reflecting the losses of ethene isotopomers

<sup>5</sup>  $E_a = 69 \text{ kJ mol}^{-1}$  has been determined for the 1,2-CH<sub>3</sub> shift in heptamethylbenzenium ions [43,44].

<sup>6</sup>  $\Delta H_f([1 + H]^+) = 745 \text{ kJ mol}^{-1}$ ,  $\Delta H_f(p\text{-CH}_3\text{C}_6\text{H}_4^+) = 1057 \text{ kJ mol}^{-1}$ ,  $\Delta H_f(CH_4) = -75 \text{ kJ mol}^{-1}$ .



Scheme 4. Composite scrambling prior to methane loss from metastable *para*-xylum ions  $[1 + H]^+$ .

from the  $^{13}\text{C}$ -labeled xylum ions  $[1\text{c} + H]^+ \rightarrow [1\text{f} + H]^+$  are shown in Fig. 4 and the data are collected in Table 4.

Similar to the elimination of methane, ethene loss from the  $^{13}\text{C}$ -labeled xylum ions indicates a rela-

Table 3

Loss of ethene from metastable xylum ions  $\text{CD}_3\text{-C}_6\text{H}_5^+ \text{-CH}_3$  ( $[1\text{a} + H]^+$ )<sup>a</sup>

Entry/loss of	$\text{C}_2\text{HD}_3$	$\text{C}_2\text{H}_2\text{D}_2$	$\text{C}_2\text{H}_3\text{D}$	$\text{C}_2\text{H}_4$
Experimental <sup>b</sup>	13.4	36.3	30.4	20.0
Statistical ( $\text{H}_8/\text{D}_3$ )	2.4	25.5	50.9	21.2
Composite model (see text) <sup>c</sup>	12.2	35.7	31.9	20.2

<sup>a</sup> Data given in %  $\Sigma$ .

<sup>b</sup> Precursor ion:  $4\text{a}^{*+}$ .

<sup>c</sup> Calculated on the basis of the  $^{13}\text{C}$ -labeling results.

tively high degree of specificity. The  $[\alpha\text{-}^{13}\text{C}]$ -labeled ions  $[1\text{c} + H]^+$  eliminate  $^{13}\text{C}^{12}\text{CH}_4$  and  $^{12}\text{C}_2\text{H}_4$  in similar amounts (45:55). Neither an assumed truly “specific” incorporation of two originally adjacent carbon atoms, i.e.,  $\text{C}^{\alpha}$  and  $\text{C}^{\text{ipso}}$  as well as  $\text{C}^{\alpha'}$  and  $\text{C}^{\text{isop}'}\text{'}$ , into the  $\text{C}_2\text{H}_4$  neutral (50:50), nor the specific loss of one  $\text{C}^{\alpha}$  atom together with one of the other seven tolyl C atoms at random (57.1:42.9), nor the completely statistical incorporation (25:75) can explain the experimental data. The  $[\alpha,\alpha\text{-}^{13}\text{C}_2]$  isotopomer  $[1\text{d} + H]^+$  expels mainly the singly labeled neutral  $^{13}\text{C}^{12}\text{CH}_4$  (76–78%); however, the losses of  $^{13}\text{C}_2\text{H}_4$  (9–11%) and  $^{12}\text{C}_2\text{H}_4$  (12–14%) are also observed. These data are also in strong disagreement with the three simple assumptions mentioned above.

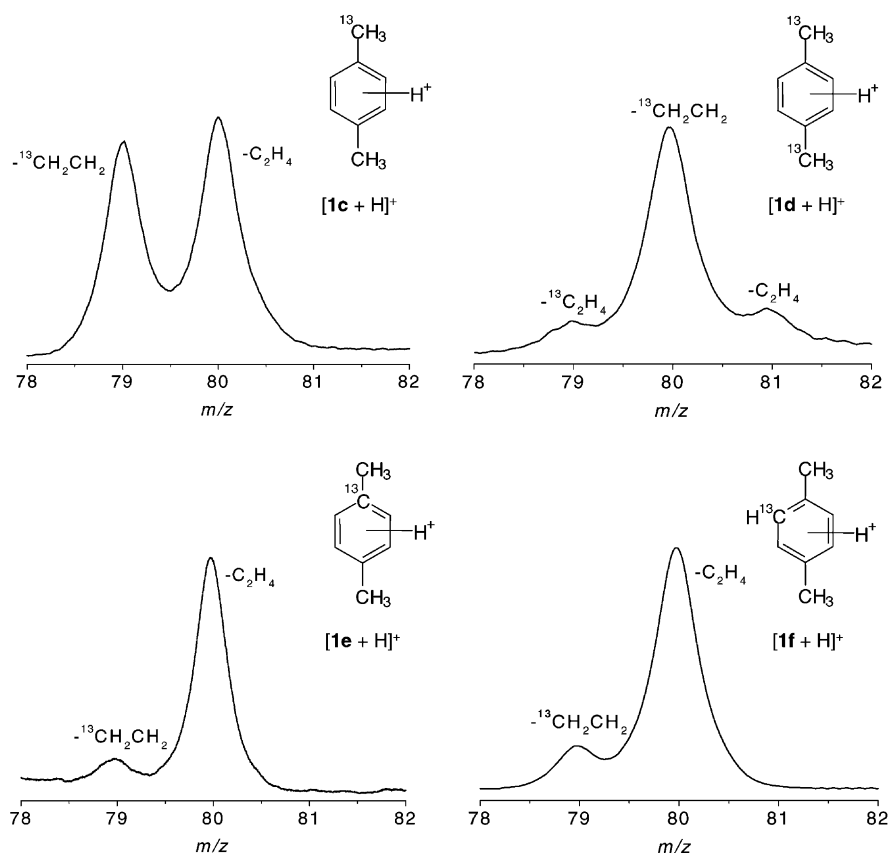


Fig. 4. Partial MIKE spectra of the  $^{13}\text{C}$ -labeled xylenium ions  $[1\text{c} + \text{H}]^+$ – $[1\text{f} + \text{H}]^+$  showing the loss of ethene. Ions  $[1\text{c} + \text{H}]^+$  were generated by EI of methyl 1- $^{13}\text{C}$  methyl-4-methyl-1,4-dihydrobenzoate (**5c**), whereas ions  $[1\text{d} + \text{H}]^+$ – $[1\text{f} + \text{H}]^+$  were generated by CI( $\text{CH}_4$ ) from the corresponding  $^{13}\text{C}$ -labeled xylenes.

Most interestingly, the two [ring- $^{13}\text{C}$ ]-labeled isotopomers  $[1\text{e} + \text{H}]^+$  and  $[1\text{f} + \text{H}]^+$  exhibit identical MIKE spectra within the limits of experimental error, with predominant loss of  $^{12}\text{C}_2\text{H}_4$  (ca. 86%) but significant contributions of  $^{13}\text{C}^{12}\text{CH}_4$  (ca. 14%). This latter finding clearly indicates, in particular through the data of ions  $[1\text{f} + \text{H}]^+$ , that the original  $\text{C}^\alpha\text{--C}^{\text{ipso}}$  bonds of the xylenium ions do not persist and there is no selectivity left with regard to the ring position of the carbon atoms expelled with the ethene fragment. Fast 1,2- $\text{CH}_3$  shifts in the xylenium ions and/or in a ring-expanded isomer, mentioned above, can explain this finding.

The combined experimental evidence of the  $^{13}\text{C}$ -labeling indicates that, here again, metastable

xylenium ions  $[1 + \text{H}]^+$  behave as fractions of ions, each of which undergoes different isomerization processes prior to fragmentation. Thus, “composite scrambling” models were tested to simulate the observed abundance distributions of ethene isotopomers. Satisfactory agreement with *all* of the experimental data is obtained by assuming that 75% of the xylenium ions  $[1 + \text{H}]^+$  undergo the specific, irreversible ring expansion to methylidihydrotrypilium ions  $[2 + \text{H}]^+$  and subsequent recontraction to ethylbenzenium isomers  $[3 + \text{H}]^+$  (Scheme 5). Fast 1,2-shifts of the methyl groups along the benzenium ring and/or the seven-membered ring are included. The remaining fraction (25%) of ions  $[1 + \text{H}]^+$  is assumed to undergo *reversible* ring expansion/recontraction via ions

Table 4

Loss of ethene from metastable  $^{13}\text{C}$ -labeled xylenium ions  $[\mathbf{1c} + \text{H}]^+ - [\mathbf{1f} + \text{H}]^+ \text{ }^{\text{a}}$ 

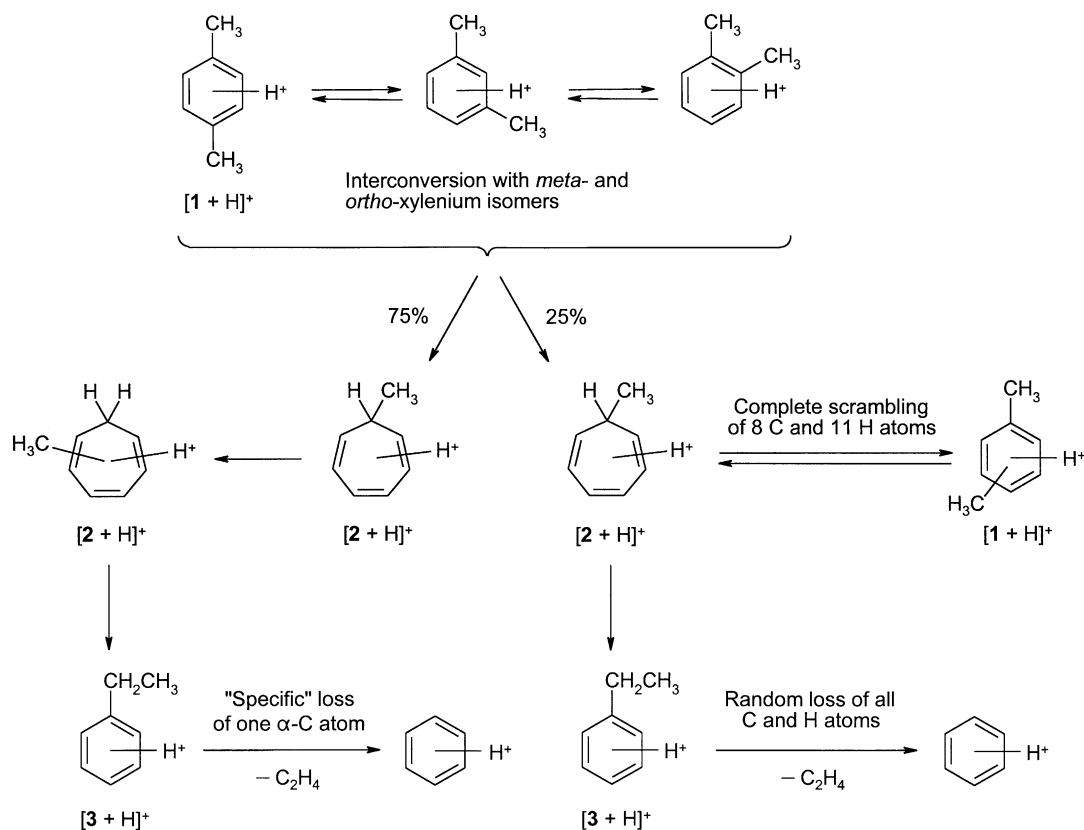
Ion		Neutral precursor	Loss of $^{13}\text{C}_2\text{H}_4$	Loss of $^{13}\text{C}^{12}\text{CH}_4$	Loss of $^{12}\text{C}_2\text{H}_4$
$^{13}\text{CH}_3\text{-C}_6\text{H}_5^+ \text{-CH}_3$ $[\mathbf{1c} + \text{H}]^+$	Exp'1	<b>5c</b> (EI)	–	<b>45.4</b>	<b>54.6</b>
Specific loss of $\text{C}^\alpha$ and adjacent $\text{C}^{\text{ipso}}$			–	50.0	50.0
Specific loss of $\text{C}^\alpha$ or $\text{C}^{\alpha'}$ with statistical loss from the remaining $\text{C}_7$ unit			–	57.1	42.9
Statistical loss ( $^{13}\text{C}_1/^{12}\text{C}_7$ )			–	25.0	75.0
Composite model (see text) <sup>b</sup>			–	43.8	56.3
Refined model (see text) <sup>b,c</sup>			–	44.6	55.4
$^{13}\text{CH}_3\text{-C}_6\text{H}_5^+ \text{-}^{13}\text{CH}_3$ $[\mathbf{1d} + \text{H}]^+$	Exp'1	<b>5d</b> (EI) <b>1d</b> (CI)	<b>9.4</b> <b>10.8</b>	78.3 75.6	12.3 13.6
Specific loss of $\text{C}^\alpha$ and adjacent $\text{C}^{\text{ipso}}$			0	100.0	0
Specific loss of $\text{C}^\alpha$ or $\text{C}^{\alpha'}$ with statistical loss from the remaining $\text{C}_7$ unit			14.3	85.7	0
Statistical loss ( $^{13}\text{C}_2/^{12}\text{C}_6$ )			3.6	42.8	53.6
Composite model (see text) <sup>b</sup>			11.6	75.0	13.4
Refined model (see text) <sup>b,c</sup>			11.8	74.0	14.2
$[1\text{-}^{13}\text{C}]\text{-}\{\text{CH}_3\text{-C}_6\text{H}_5^+ \text{-CH}_3\}$ $[\mathbf{1e} + \text{H}]^+$	Exp'1	<b>1e</b> (CI)	–	<b>13.5</b>	<b>86.5</b>
Specific loss of $\text{C}^\alpha$ and adjacent $\text{C}^{\text{ipso}}$			–	0	100.0
$[2\text{-}^{13}\text{C}]\text{-}\{\text{CH}_3\text{-C}_6\text{H}_5^+ \text{-CH}_3\}$ $[\mathbf{1f} + \text{H}]^+$	Exp'1	<b>1f</b> (CI)	–	<b>14.1</b>	<b>85.9</b>
Specific loss of $\text{C}^\alpha$ and adjacent $\text{C}^{\text{ipso}}$			–	100.0	0
Specific loss of $\text{C}^\alpha$ or $\text{C}^{\alpha'}$ with statistical loss from the remaining $\text{C}_7$ unit			–	14.3	85.7
Statistical loss ( $^{13}\text{C}_1/^{12}\text{C}_7$ )			–	25.0	75.0
Composite model (see text) <sup>b</sup>			–	17.0	83.0
Refined model (see text) <sup>b,c</sup>			–	15.6	84.4

<sup>a</sup> Data given in %  $\Sigma$ .<sup>b</sup> Calculated for composite scrambling (75% “specific”, 25% statistical).<sup>c</sup> Calculated for composite scrambling (66% “specific”, 34% iteratively statistical).

$[\mathbf{2} + \text{H}]^+$  leading to complete carbon scrambling prior to the final ring contraction to ethylbenzenium ions  $[\mathbf{3} + \text{H}]^+$ . This mixture of two fractions of different isomerization behavior explains, within the limits of experimental error, the two minor contributions of  $^{13}\text{C}_2\text{H}_4$  (11%) and  $^{12}\text{C}_2\text{H}_4$  (14%) observed for ions  $[\mathbf{1d} + \text{H}]^+$  and also the ratio of 45:55 found for the losses of  $^{13}\text{C}^{12}\text{CH}_4$  and  $^{12}\text{C}_2\text{H}_4$  from ions  $[\mathbf{1c} + \text{H}]^+$  (Table 4).

A slight deviation from the experimental data remains for the [ring- $^{13}\text{C}$ ]-labeled isotopomers  $[\mathbf{1e} + \text{H}]^+$  and  $[\mathbf{1f} + \text{H}]^+$ ; however, the discrepancy of 3% can be diminished by assuming, instead of the “black and white” (75% partially “specific” vs. 25% random) behavior, a still somewhat more re-

alistic situation. In that final model, the fraction of ions  $[\mathbf{1} + \text{H}]^+$  which undergo the irreversible ring expansion/contraction is reduced to 66%, but the remaining one (34%) is assumed to behave fractionally itself: after a single ring expansion/contraction, an (again) 66%-fraction of these ions reacts irreversibly to ethylbenzenium ions  $[\mathbf{3} + \text{H}]^+$  to eliminate ethene, whereas the remaining fraction undergoes another ring expansion/contraction cycle via the methylidihydrotropylium isomer  $[\mathbf{2} + \text{H}]^+$ . Repeated steps of this fractionally reversible and irreversible skeletal isomerization gradually increase the simulated contribution of the  $^{12}\text{C}_2\text{H}_4$  loss from ions  $[\mathbf{1e} + \text{H}]^+$  and  $[\mathbf{1f} + \text{H}]^+$  (Table 4) and, within experimental error, render it identical with the experimentally determined one.



Scheme 5. Composite scrambling prior to ethene loss from metastable *para*-xylenium ions  $[1 + H]^+$ .

The model developed to explain the composite carbon scrambling in ions  $[1 + H]^+$  was found to be perfectly suitable to understand the extent of H/D scrambling in the  $[\alpha, \alpha, \alpha\text{-D}_3]$ -labeled ions  $[1a + H]^+$  (Fig. 2). It is sufficient to assume that the two fractions of ions, which undergo irreversible (75%) and reversible (25%) ring expansion/recontraction as discussed above, generate the corresponding mixture of  $[D_3]$ -ethylbenzenium ions containing the label according to the skeletal rearrangement. These  $[D_3]$ -ethylbenzenium intermediates eliminate the  $C_2(H,D)_4$  isotopomers in the manner known for metastable ethylbenzenium ions (viz.  $C_6H_6CH_2CD_3$  and  $C_6H_6CD_2CH_3$ ) [39]. For example, putative ions  $C_6H_5D\text{-CHD-CH}_2D$  would be assumed to completely retain the ring-D atom in the product ions

generated by losses of  $C_2H_3D$  and  $C_2H_2D_2$  and retain the  $\alpha$ -D atom with the probability  $p = 0.07$  and the  $\beta$ -D atom with  $p = 0.23$  [39]. The pattern of  $C_2(H,D)_4$  losses calculated in this manner on the basis of the C-scrambling data match the experimentally determined distribution within experimental error (Table 4). Further refinement of the model, as described above for the carbon scrambling, is not necessary.

Our simulation of the composite scrambling behavior of metastable xylenium ions  $[1 + H]^+$  prior to ethene loss appears to be a valid approach. It clearly reflects the energy-demanding ring expansion of the metastable xylenium ions to methylidihydrotropylium ions  $[2 + H]^+$  and the competition between the ring expansion of the latter ions back to the protonated



xylenes and forward to protonated ethylbenzene  $[3 + H]^+$ , from which ethene can be expelled relatively easily. In fact, the predominance of the ethene loss from metastable protonated methylcycloheptatriene  $[2 + H]^+$ , which was found to occur *without* the intermediacy of xylenium ions [37], has demonstrated that irreversible ring contraction to protonated ethylbenzene  $[3 + H]^+$  is the strongly preferred ring contraction path of this protonated polyolefin [46].

#### 4. Conclusion

Protonated methylbenzenes undergo complex isomerization reactions prior to unimolecular fragmentation on the microsecond timescale. As shown in detail in this study, metastable xylenium ions generated either by protonation of *para*-xylene in the plasma of a  $Cl(CH_4)$  source or by directed, EI-induced fragmentation of 1,4-dimethyl-1,4-dihydrobenzoic acid or its methyl ester, react in a similarly complex manner as do metastable toluenium ions (protonated toluene) [15]. Loss of methane from xylenium ions occurs mainly by protonolysis of the  $C^\alpha-C^{ipso}$  bonds with a high degree of carbon-specificity (ca. 92%), accompanied by slow hydrogen exchange between the methyl groups and the ring ( $H^\alpha/H^{ring}$  scrambling). A minor fraction (ca. 8%) of the ions undergo complete scrambling of the eight carbon and 11 hydrogen atoms. This “composite scrambling” behavior [6] is similar to the isomerization of toluenium ions but the fraction of ions reacting specifically is markedly increased. It may be argued that the tendency to generate nonclassical intermediates, such as the carbonium ions  $\{[1 + H]^+\}'$  and  $\{[1 + H]^+\}''$  (cf. Scheme 2), is reduced with more electron rich arenium ions. The intermediacy of pentacoordinate carbocations of this type during the fragmentation of protonated methylbenzenes may be a key to those heterolytic C–C bond cleavages which cannot involve a hydrogen transfer from a remote ( $\beta$  or more distant) position, which is known, for example, for the loss of alkenes from protonated higher alkylbenzenes. Isomerization

by methyl ring walk (1,2- $CH_3$  shifts) has been assumed to precede the methane loss from xylenium ions.

An additional and particularly “diagnostic” fragmentation path of metastable xylenium ions is the loss of ethene. This reaction occurs after ring expansion to protonated methylcycloheptatriene (methyldihydrotropylium ions) and subsequent re-contraction to protonated ethylbenzene (ethylbenzenium ions), from which the olefin is expelled. However, ethene loss is also preceded by composite scrambling. The major fraction of ions (66–75%) react by scrambling of seven carbon atoms and eight hydrogen atoms—excluding one of the methyl carbons—which is expelled “specifically” with the ethene fragment. 1,2- $CH_3$  shifts occur on the level of the xylenium and/or the methyldihydrotropylium ions. A minor fraction of the xylenium ions (34–25%) undergoes complete carbon and hydrogen scrambling by reversible ring expansion/contraction, thus repeatedly regenerating the methyldihydrotropylium isomers prior to the eventual formation of ethylbenzenium ions.

In conclusion, it has been demonstrated that the complex isomerization behavior of long-lived xylenium ions prior to unimolecular fragmentation can be understood by using extended  $^{13}C$ -labeling, in addition to  $^2H$ -labeling. In this view, insight into the composite scrambling processes of these small and apparently simple methylbenzenium ions has been developed to a satisfactory degree of confidence.

#### Acknowledgements

We thank Professor Charles H. DePuy for having communicated his unpublished results on the fragmentation of  $C_7H_9^+$  and  $C_8H_{11}^+$  ions [36] to us. We also thank Dr. Gerald Prior and Dr. Anja Barkow for their early contributions to this project. D.K. is indebted to the Fonds der Chemischen Industrie (Frankfurt/Main) for financial support and M.M. gratefully acknowledges financial support by the Graduiertenförderung des Landes Nordrhein-Westfalen.

## References

- [1] R. Taylor, *Electrophilic Aromatic Substitution*, Wiley, Chichester, 1990.
- [2] S. Fornarini, *Mass Spectrom. Rev.* 15 (1996) 365.
- [3] S. Fornarini, M.E. Crestoni, *Acc. Chem. Res.* 31 (1998) 827.
- [4] A.G. Harrison, *Chemical Ionization Mass Spectrometry*, 2nd Edition, CRC Press, Boca Raton, FL, 1992, Chapter 5, p. 113.
- [5] (a) D. Kuck, *Mass Spectrom. Rev.* 9 (1990) 583;  
(b) D. Kuck, *Mass Spectrom. Rev.* 9 (1990) 181.
- [6] D. Kuck, *Int. J. Mass Spectrom.* 213 (2002) 101.
- [7] J.A. Herman, A.G. Harrison, *Org. Mass Spectrom.* 16 (1981) 423.
- [8] J.P. Denhez, H.E. Audier, D. Berthomieu, *Org. Mass Spectrom.* 28 (1993) 704.
- [9] C. Wesdemiotis, H. Schwarz, C.C. Van de Sande, F. Van Gaever, *Z. Naturforsch.* 34b (1979) 495.
- [10] J. Hrušák, D. Schröder, T. Weiske, H. Schwarz, *J. Am. Chem. Soc.* 115 (1993) 2015.
- [11] (a) H.E. Audier, C. Monteiro, P. Mourgues, D. Berthomieu, *Org. Mass Spectrom.* 25 (1990) 245;  
(b) D. Berthomieu, V. Brenner, G. Ohanessian, J.P. Denhez, P. Millié, H.E. Audier, *J. Phys. Chem.* 99 (1995) 712;  
(c) J.P. Denhez, H.E. Audier, D. Berthomieu, *Rap. Commun. Mass Spectrom.* 9 (1995) 1210.
- [12] C. Matthias, S. Anlauf, K. Weniger, D. Kuck, *Int. J. Mass Spectrom.* 199 (2000) 155.
- [13] (a) D. Kuck, C. Matthias, *J. Am. Chem. Soc.* 114 (1992) 1901;  
(b) C. Matthias, D. Kuck, *Org. Mass Spectrom.* 28 (1993) 1073;  
(c) C. Matthias, K. Weniger, D. Kuck, *Eur. Mass Spectrom.* 1 (1995) 445;  
(d) C. Matthias, D. Kuck, *Int. J. Mass Spectrom.* 217 (2002) 131.
- [14] (a) D.H. Williams, G. Hvistendahl, *J. Am. Chem. Soc.* 96 (1974) 6755;  
(b) G. Hvistendahl, D.H. Williams, *J. Chem. Soc., Perkin Trans. 2* (1975) 881.
- [15] D. Kuck, J. Schneider, H.-F. Grützmacher, *J. Chem. Soc., Perkin Trans. 2* (1985) 689.
- [16] D. Kuck, G. Prior, H.-F. Grützmacher, D.R. Müller, W.J. Richter, *Adv. Mass Spectrom.* 11A (1989) 750.
- [17] A.G. Harrison, P.H. Lin, H.W. Leung, *Adv. Mass Spectrom.* 7B (1978) 1394.
- [18] K. Iseda, *Chem. Bull. Soc. Jpn.* 51 (1978) 2167.
- [19] V.D. Nefedov, E.N. Sinotova, G.P. Akulov, M.V. Korsakov, *J. Org. Chem. USSR* 6 (1970) 1220.
- [20] H.H. Büker, H.-F. Grützmacher, M.E. Crestoni, A. Ricci, *Int. J. Mass Spectrom. Ion Process.* 160 (1997) 167.
- [21] D. Kuck, D.R. Müller, W.J. Richter, unpublished results.
- [22] Z. Szilágyi, K. Vékey, *Eur. Mass Spectrom.* 1 (1995) 507.
- [23] K. Tamao, K. Sumitani, M. Kumada, *J. Am. Chem. Soc.* 94 (1972) 4374.
- [24] (a) M. Fields, M.A. Leaffer, J. Rohan, *Science* 109 (1949) 35;  
(b) M. Fields, M.A. Leaffer, S. Rothschild, J. Rohan, *J. Am. Chem. Soc.* 74 (1952) 5498.
- [25] A.V. Robertson, C. Djerassi, *J. Am. Chem. Soc.* 90 (1968) 6992.
- [26] M. Mormann, D. Kuck, *J. Label. Comp. Radiopharm.* 45 (2002) 601.
- [27] H. van Bekkum, C.B. van den Bosch, G. van Minnen-Pathuis, J.C. de Mos, A.M. van Wijk, *Rec. Trav. Chim. Pays-Bas* 90 (1971) 137.
- [28] J.H. Brewster, H.O. Bayer, S.F. Osman, *J. Org. Chem.* 29 (1964) 110.
- [29] A.P. Terentyev, L.I. Belenky, L.A. Yanovskaya, *Z. Obsh. Khim.* 24 (1954) 1251.
- [30] H. Gilman, W. Langham, F.W. Moore, *J. Am. Chem. Soc.* 62 (1949) 2327.
- [31] D. Kuck, W. Bähler, H.-F. Grützmacher, *J. Am. Chem. Soc.* 101 (1979) 7154.
- [32] (a) F.H.W. van Amerom, W.J. van der Hart, N.M.M. Nibbering, *Int. J. Mass Spectrom.* 182/183 (1999) 7;  
(b) F.H.W. van Amerom, D. van Duijn, W.J. van der Hart, N.M.M. Nibbering, *J. Am. Soc. Mass Spectrom.* 12 (2001) 359.
- [33] (a) E.L. Øiestad, Å.M.L. Øiestad, H. Skaane, K. Ruud, T. Helgaker, E. Uggerud, T. Vulpus, *Eur. Mass Spectrom.* 1 (1995) 121;  
(b) E.L. Øiestad, E. Uggerud, *Int. J. Mass Spectrom. Ion Process.* 165/166 (1997) 39;  
(c) Å.M.L. Øiestad, E. Uggerud, *Int. J. Mass Spectrom. Ion Process.* 167/168 (1997) 117;  
(d) E.L. Øiestad, E. Uggerud, *Int. J. Mass Spectrom.* 199 (2000) 91.
- [34] D.J. Swanton, D.C.J. Marsden, L. Radom, *Org. Mass Spectrom.* 26 (1991) 227.
- [35] (a) R. Gareyev, T.J. DePuy, V.M. Bierbaum, C.H. DePuy, *Int. J. Mass Spectrom.* 179/180 (1998) 55;  
(b) C.H. DePuy, R. Gareyev, J. Hankin, G.E. Davico, M. Krempp, R. Damrauer, *J. Am. Chem. Soc.* 120 (1998) 5086.
- [36] E. Motell, M.S. Robinson, R. Gareyev, V.M. Bierbaum, C.H. DePuy, unpublished results.
- [37] M. Mormann, D. Kuck, *J. Mass Spectrom.* 34 (1999) 384.
- [38] (a) M. Mormann, D. Kuck, *Int. J. Mass Spectrom.* 210/211 (2001) 531;  
(b) M. Mormann, Doctoral Thesis, Universität Bielefeld, 2000.
- [39] H.E. Audier, C. Monteiro, D. Robin, *New J. Chem.* 13 (1989) 621.
- [40] H.E. Audier, G.K. Koyanagi, T.B. McMahon, D. Thölmann, *J. Phys. Chem.* 100 (1996) 8220.
- [41] H.E. Audier, F. Dahhani, A. Milliet, D. Kuck, *J. Chem. Soc., Chem. Commun.* (1997) 429.
- [42] N.S. Isaacs, *Physical Organic Chemistry*, Longman, Harlow, 1987, p. 255.
- [43] G.I. Borodkin, S.M. Nagy, V.I. Mahatyuk, M.M. Shakirov, V.G. Shubin, *J. Chem. Soc., Chem. Commun.* (1983) 1533.

- [44] P. Vogel, Carbocation Chemistry, Elsevier, Amsterdam, 1985, pp. 142, 323.
- [45] (a) T. Baer, J.C. Morrow, J.D. Shao, S. Olesik, J. Am. Chem. Soc. 110 (1988) 5633;  
(b) S.G. Lias, J.E. Bartmess, J.F. Liebman, J.L. Holmes, R.D. Levin, W.G. Mallard, J. Phys. Chem. Ref. Data 17 (Suppl. 1) (1998);  
(c) W.G. Mallard, P.J. Linstrom (Eds.), NIST Chemistry Webbook, NIST Standard Reference Database No. 69, March 1998, National Institute of Standards and Technology, Gaithersburg, MD (<http://webbook.nist.gov>).
- [46] D. Kuck, M. Mormann, in: Z. Rappoport (Ed.), The Chemistry of Functional Groups: The Chemistry of Dienes and Polyenes, Vol. 2, Wiley, New York, 2000, p. 1.